

VITA: Variational Pretraining of Transformers for Climate-Robust Crop Yield Forecasting

Adib Hasan Mardavij Roozbehani Munther Dahleh

Massachusetts Institute of Technology

{notadib, mardavij, dahleh}@mit.edu

Abstract

Accurate crop yield forecasting is essential for global food security. However, current AI models systematically underperform when yields deviate from historical trends. We attribute this to the lack of rich, physically grounded datasets directly linking atmospheric states to yields. To address this, we introduce *VITA (Variational Inference Transformer for Asymmetric data)*, a variational pretraining framework that learns representations from large satellite-based weather datasets and transfers to the ground-based limited measurements available for yield prediction. VITA is trained using detailed meteorological variables as proxy targets during pretraining and learns to predict latent atmospheric states under a seasonality-aware sinusoidal prior. This allows the model to be fine-tuned using limited weather statistics during deployment. Applied to 763 counties in the U.S. Corn Belt, VITA achieves state-of-the-art performance in predicting corn and soybean yields across all evaluation scenarios, particularly during extreme years, with statistically significant improvements (paired t-test, $p < 0.0001$). Importantly, VITA outperforms prior frameworks like GNN-RNN without soil data, and bigger foundational models (e.g., Chronos-Bolt) with less compute, making it practical for real-world use—especially in data-scarce regions. This work highlights how domain-aware AI design can overcome data limitations and support resilient agricultural forecasting in a changing climate.

Introduction

Climate change is transforming agriculture, with extreme weather causing billions in annual crop losses (Lobell, Schlenker, and Costa-Roberts 2011). In 2012, U.S. drought reduced corn yields by 13%, while 2019 flooding prevented planting on 19.4 million acres (USDA National Agricultural Statistics Service 2013; USDA Farm Service Agency 2019). Accurate yield prediction under such volatility is critical for agricultural risk management and long-term food security (Beddington 2010). Yet current operational models—including regression-based approaches from USDA ERS (Westcott and Jewison 2013) and USDA NASS (NASS 2023)—often fail when yields diverge from historical trends.

The challenge stems from fundamental data limitations of existing methods in yield forecasting. First, many models train on less than 10 years of historical data (Gandhi, Petkar, and Armstrong 2016; Lin et al. 2024), insufficient for capturing rare but increasingly critical extreme weather patterns.

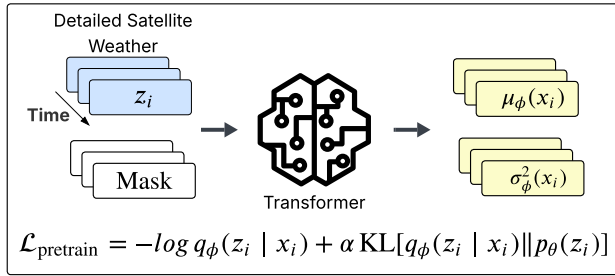
Second, multi-modal approaches (You et al. 2017; Lin et al. 2024; Khaki, Wang, and Archontoulis 2019; Fan et al. 2021) rely on extensive auxiliary data—satellite imagery, soil surveys, planting records, and weather records—which limits their applicability in regions that lack detailed agricultural monitoring infrastructure.

Third, general-purpose time-series pretraining methods like SimMTM (Dong et al. 2023), PatchTST (Wu et al. 2023), and foundational models, such as, Chronos (Ansari et al. 2024) assume consistent input features between pretraining and fine-tuning. This is suboptimal weather domains, where pretraining can leverage rich satellite datasets with dozens of variables (e.g., 31 meteorological variables from NASA POWER (NASA 2024)), but fine-tuning must rely on smaller, accessible subsets (e.g., 6 basic weather variables from Khaki, Wang, and Archontoulis (2019)). We term this the *data asymmetry problem*, in which pretraining and operational feature sets fundamentally differ—an issue largely unaddressed by existing AI approaches.

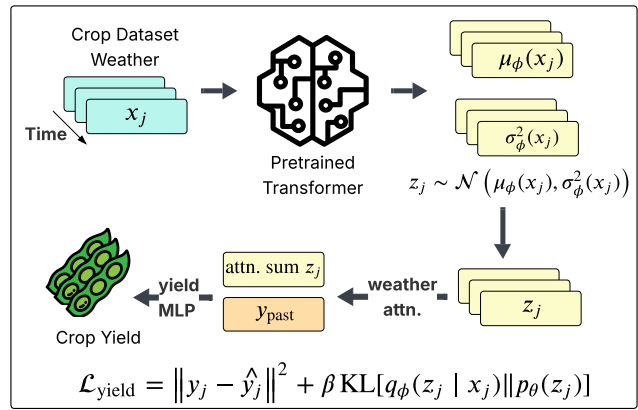
To overcome this limitation, we introduce VITA, a variational pretraining framework for weather–yield prediction that transfers knowledge from rich satellite data to limited ground-based inputs. Trained with a variational loss and feature mask, VITA learns latent weather representations that generalize to settings with fewer variables. Since many crop yields are largely governed by weather, this objective enables rich representation learning essential for yield forecasting.

Unlike a standard variational autoencoder (VAE) (Kingma and Welling 2013), VITA is trained without a decoder – it maximizes the variational likelihood using detailed weather variables as proxy targets, with a sinusoidal prior to capture seasonality. During fine-tuning, six years of historical yield serve as a proxy for soil and management factors, reducing data requirements. In total, VITA adds under 2% more parameters than a standard Transformer encoder (Vaswani et al. 2017) and trains end-to-end in under 2.5 hours on a single L40S GPU. Its efficiency and exclusive reliance on public data (NASA POWER, USDA yield) make it practical for operational use, including crop insurance and subsidy programs.

Empirically, VITA delivers state-of-the-art accuracy, particularly in years with extreme yield deviations, with statistically significant gains ($p < 0.0001$) over other pretrain-



(a) Variational pretraining



(b) Yield prediction fine-tuning

Figure 1: Two-stage variational training framework for asymmetric weather features. (a) A transformer encoder is pretrained on 31-variable weather time series by randomly masking $10 \leq k \leq 25$ features and predicting them from remaining context. The model learns a variational posterior $q_\phi(z_i | x_i)$ over weather representations by directly maximizing variational likelihood. (b) During fine-tuning, only 6 weather features are available. The pretrained transformer encodes these into a latent distribution $q_\phi(z_j | x_j)$, from which $z_j \sim \mathcal{N}(\mu_\phi(x_j), \sigma_\phi^2(x_j))$ is sampled. It is aggregated with learnable attention across time dimension and concatenated with historical yield y_{past} for final yield prediction.

ing strategies. It also generalizes strongly across space and time—models pretrained on non-U.S. weather improve U.S. fine-tuning, and those trained on 1994–2009 remain accurate for 2014–2018—demonstrating robust, transferable weather representations.

In summary, the key contributions of this work are:

- A decoder-free variational pre-training framework for modeling asymmetric features (see Equation 8).
- A seasonality-aware sinusoidal prior that captures structured temporal patterns.
- State-of-the-art performance in years with extreme yield deviations, validated through rigorous, statistically grounded evaluation.

The remainder of this paper is organized as follows: Related Work reviews prior methods; Methodology details our variational framework, Experiments presents our experimental setup, Results analyzes performance across various conditions, and Discussion discusses implications and limitations.

Related Work

Crop Yield Prediction. Researchers have proposed various different approaches to for crop yield forecasting, including mechanistic modeling, CNN-RNN architectures, graph neural networks, Deep Gaussian Processes, and Vision Transformers (Keating et al. 2003; Khaki, Wang, and Archontoulis 2019; Fan et al. 2021; You et al. 2017; Lin et al. 2024). Multi-modal approaches integrate satellite imagery, weather data, soil surveys, management records, and vegetation indices (Wu et al. 2021; Sun et al. 2019; Gandhi, Petkar, and Armstrong 2016; Oliveira et al. 2018; Basir et al. 2021;

Hasan, Roozbehani, and Dahleh 2024; Ferraz et al. 2024; Cao, Ma, and Zhang 2022). However, extensive data requirements limit deployment in regions with limited agricultural monitoring infrastructure, and many approaches rely on temporally short regional datasets that may not capture sufficient weather variability for extreme events (Gandhi, Petkar, and Armstrong 2016; Lin et al. 2024; McFarland et al. 2020; Chu and Yu 2020).

Time Series Pretraining. Recent work develops unsupervised representation learning through contrastive methods, transformer frameworks, and masked reconstruction (Franceschi, Dieuleveut, and Jaggi 2019; Yue et al. 2022; Zerveas et al. 2021; Dong et al. 2023; Wu et al. 2023; Woo et al. 2022). These methods achieve strong forecasting performance but do not explicitly model data asymmetry, which is critical for weather based yield forecasting.

Variational Methods. Variational autoencoders and have been applied to weather prediction, climate forecasting, and agricultural data generation (Kingma and Welling 2013; Higgins et al. 2017; Kwok and Qi 2021; Wang et al. 2024; Palma et al. 2025; Razavi et al. 2024). However, existing variational methods are not used for asymmetric data learning. Our work is applicable for this particular problem and learns latent state without input reconstruction and with a seasonality-aware sinusoidal prior.

Methodology

VITA incorporates a two-stage approach: (1) self-supervised pretraining on extensive weather data to learn robust weather representations, and (2) variational fine-tuning with basic weather statistics and past yields.

Problem Formulation

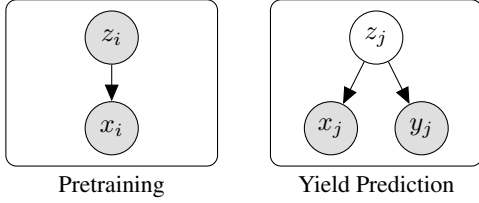


Figure 2: Graphical model depicting data structure of pretraining and prediction phases in VITA.

We formulate crop yield prediction as semi-supervised learning with latent weather representations. Suppose $z \in \mathbb{R}^{364 \times 31}$ denotes the detailed meteorological variables from pretraining, and $x \in \mathbb{R}^{364 \times 6}$ denotes basic weather statistics (temperature, precipitation, etc.) available in both pretraining and downstream tasks. Each weather input is a 364-week sequence representing seven years of weekly means.

We consider two datasets: (1) a pretraining dataset $\mathcal{D}_w = \{(x_i, z_i)\}_{i=1}^{N_w}$, where both basic and detailed weather states are observed for each 364-week *non-overlapping* window i across the NASA POWER grid, but no yield information is available; and (2) a finetuning dataset $\mathcal{D}_y = \{(x_j, y_j, y_{\text{past},j})\}_{j=1}^{N_y}$, where detailed states z_j remain latent for each 364-week *overlapping* sequence j across U.S. Corn Belt counties. Each training example uses weather from years $[t-6, t]$ and historical yields from $[t-6, t-1]$ to predict yield $y_{c,t}$ for county c . Test-year yields are strictly held out during training and additional details are provided in the Appendix. We model each county independently as a 1D temporal sequences and spatial context enters only via (latitude, longitude) features concatenated to each timestep (Equation 1).

Architecture

VITA employs a transformer encoder that maps 364-week weather sequences into latent representations for yield prediction. The forward process is:

$$x_{\text{input}} = \text{concat}(x_{\text{weather}}, \text{year}, \text{coordinates}) \quad (1)$$

$$h_{\text{weather}} = E_{\phi}(\text{LinearProj}(x_{\text{input}}) + \text{PosEmbed}(\cdot)) \quad (2)$$

$$[\mu, \log \sigma^2] = \text{LinearProj}_{\mu, \sigma^2}(h_{\text{weather}}) \quad (3)$$

$$z = \mu + \sigma \odot \epsilon, \quad \epsilon \sim \mathcal{N}(0, I) \quad (4)$$

$$z_{\text{agg}} = \sum_{k=1}^{364} \alpha_k z_k; \quad \alpha_k = \text{softmax}(\text{MLP}_a(z_k)) \quad (5)$$

$$\hat{y}_t = \text{MLP}_y([z_{\text{agg}}, y_{\text{past},t}]) \quad (6)$$

Here, E_{ϕ} is a transformer encoder applied to weekly weather inputs x_{input} with positional embeddings, and coordinates refer to the spatial latitude and longitude. The $\text{LinearProj}_{\mu, \sigma^2}$ outputs the mean and log-variance of each latent state; MLP_a computes attention weights for temporal

aggregation into z_{agg} ; and MLP_y maps the aggregated latent representation and historical yields to the predicted yield \hat{y}_t .

Self-Supervised Pretraining

We pretrain on NASA POWER dataset (1984-2022) using progressive feature-wise masking, starting with $k = 10$ masked features and increasing by 1 every 2 epochs until 25 out of 31 features are masked. The pretraining objective balances reconstruction with regularization:

$$\begin{aligned} \mathcal{L}_{\text{pretrain}} &= -\mathbb{E}_{(x_i, z_i) \sim \mathcal{D}_w} [\log q_{\phi}(z_i | x_i) \\ &\quad + \alpha \cdot \text{KL}[q_{\phi}(z_i | x_i) \| p_{\theta}(z_i)]] \\ &= -\mathbb{E}_{(x_i, z_i) \sim \mathcal{D}_w} [\log \mathcal{N}(z_i; \mu_{\phi}(x_i), \sigma_{\phi}^2(x_i))] \\ &\quad + \alpha \cdot \text{KL}[q_{\phi}(z_i | x_i) \| p_{\theta}(z_i)] \end{aligned} \quad (7)$$

The first term maximizes the Gaussian likelihood, which encourages the posterior distribution $q_{\phi}(z_i | x_i)$ to accurately predict the observed detailed weather state z_i . The second term is the regularizer preventing overfitting by imposing a prior structure.

We investigate two prior distributions: standard normal $p_{\theta}(z) \sim \mathcal{N}(0, I)$ and sinusoidal prior $p_{\theta}(z) \sim \mathcal{N}(\mu_{\text{sin}} = A \sin(\theta \cdot \text{pos} + \theta_0), \sigma^2 I)$ to capture seasonal patterns. Sinusoidal prior has additional prior parameters that are learned during both pretraining and finetuning. This prior explicitly models the periodicity in weather variables, allowing a more structured latent space.

Decoder-Free Fine-Tuning Objective

Standard semi-supervised VAEs require a decoder term $\log p(x_j | z_j)$ to model input reconstruction (Kingma et al. 2014). However, in our meteorological context, established principles like the Tetens equation, Penman-Monteith formulation, Clausius-Clapeyron equation and Stefan-Boltzmann radiation balance link basic weather statistics to the detailed atmospheric state (O. Tetens 1930; Ndulue and Ranjan 2021; Brown 1951; Murray-Tortarolo 2023), making the decoder term unnecessary.

In Appendix, we empirically validated this deterministic relationship, training a small MLP to reconstruct basic weather variables from detailed ones with near-perfect accuracy ($R^2 > 0.9999$). This enables us to model $p(x_j | z_j) \approx 1$ and derive the simplified variational objective:

$$\mathcal{L}_{\text{yield}} = \|y_j - \hat{y}_j\|^2 + \beta \cdot \text{KL}[q_{\phi}(z_j | x_j) \| p_{\theta}(z_j)] \quad (8)$$

where $\beta > 0$ is a hyperparameter. Note that the β in Equation (8) does not weaken the variational objective and the full evidence lower bound (ELBO) is still optimized. The full derivation of this objective is shown in the Appendix.

Baselines

We compare against several types of baselines. (1) *Non-deep learning methods*: OLS linear regression with agronomically-motivated features following USDA Economic Research Service (ERS) methodology (Westcott and Jewison 2013), and XGBoost (Chen and Guestrin 2016). (2) *Deep learning methods*: CNN-RNN (Khaki, Wang, and Archontoulis 2019) and GNN-RNN (Fan et al. 2021). (3)

Masked time series pretraining: SimMTM (Dong et al. 2023). (4) *Pre-trained foundational time series models:* Chronos-Bolt-tiny-9M (Ansari et al. 2024) with full fine-tuning. To isolate the effect of variational pretraining from architecture, we also include T-BERT, which is identical to VITA but trained with a standard MSE reconstruction loss. Notably, XGBoost, GNN-RNN, and CNN-RNN have access to soil data, while the pretrained transformer models and OLS do not. All models use identical 364 week windows and train-test splits.

Experiments

We test three hypotheses: (1) weather pretraining improves yield prediction on extreme weather years, (2) variational objectives with sinusoidal priors outperform standard approaches, and (3) these benefits generalize to standard years and forward temporal gaps. We evaluate on county-level corn and soybean yield prediction across 763 US Corn Belt counties.

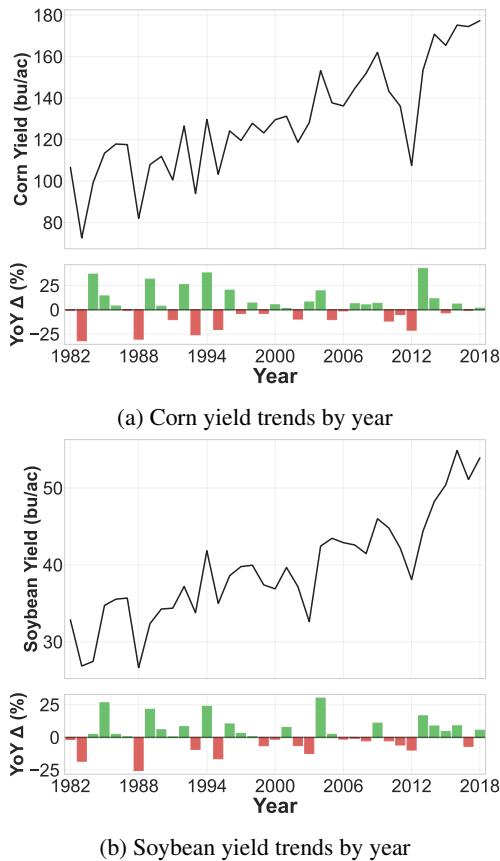


Figure 3: Mean crop yield in bushels / acre (bu/ac) 763 US Corn Belt counties showing extreme weather years as sharp deviations from historical patterns.

Data. We pretrain on the NASA POWER dataset (NASA 2024), comprising 39 years (1984–2022) of climate data at 0.5° resolution across 116 grids over the Americas. It includes 31 meteorological variables aggregated weekly

(100K sequences). However, its coarse resolution is unsuitable for county-level yield forecasting, as the median U.S. county spans 622 square miles (U.S. Census Bureau 2025). We therefore evaluate on the dataset of Khaki, Wang, and Archontoulis (2019), containing weather, soil, and county-level corn and soybean yields for 763 Corn Belt counties (1982–2018) (U.S. Department of Agriculture, National Agricultural Statistics Service 2023). Corn (C4) and soybean (C3) represent distinct physiological and weather-sensitivity regimes and jointly account for over 60% of U.S. row-crop acreage (Williams and Pounds-Barnett 2024).

The Khaki, Wang, and Archontoulis (2019) weather data include six ground-based weekly weather measurements: (1) minimum temperature, (2) maximum temperature, (3) solar radiation, (4) precipitation, (5) snow water equivalent, and (6) vapor pressure, and 11 soil properties averaged over county areas. We exclude soil data to test deployment in data-sparse regions. This presents a key challenge as pretraining contains satellite measurement of 31 meteorological variables, while fine-tuning uses only 6 ground-based variables averaged over county areas.

Training Configuration. Full hyperparameters, schedules, and data splits are detailed in Appendix 4; all models share identical splits and computational budgets. All experiments, including pretraining and grid search, share random seed 1234, unless otherwise noted.

Hyperparameter Optimization. We performed a 27-configuration grid search to optimize hyperparameters, with full details and robustness analysis in Appendix Figure 6. Best hyperparameters are used for all subsequent experiments.

Extreme Year Evaluation (Primary Contribution)

We identify the five most weather-extreme years for each crop between 2000 and 2018 by computing absolute z-scores from 5-year rolling means of yields. These include known drought years (2002, 2003, 2012) and years with favorable conditions and record-breaking yields (2004, 2009). (National Drought Mitigation Center, NOAA, and USDA 2025)

We also conduct an early-season forecasting experiment using our top four models (two VITA variants, T-BERT, and SimMTM) and OLS, truncating weather data at the end of July in the final year (week 30). This design mirrors operational forecasting systems such as USDA NASS (NASS 2023), which issue yield projections prior to harvest. Our OLS baseline follows the USDA Economic Research Service (ERS) framework (Westcott and Jewison 2013), which is conceptually similar to NASS models that also rely on regression-driven estimates grounded in observed weather and crop conditions. The OLS baseline normally incorporates July–August temperature and precipitation for soybean (Appendix 4), but for consistency across methods we limit it to July in this experiment.

Standard Years Generalization

To validate that extreme weather optimization doesn’t compromise standard performance, we evaluate on 2014–2018

Method	Corn R^2 (RMSE)	Soybean R^2 (RMSE)	Mean R^2
OLS	0.227 (27.7)	0.460 (7.0)	0.344
XGBoost	0.135 ± 0.033 (29.0 ± 0.6)	0.377 ± 0.039 (7.6 ± 0.2)	0.256
CNN-RNN	0.256 ± 0.030 (26.5 ± 0.5)	0.498 ± 0.023 (6.8 ± 0.2)	0.377
GNN-RNN	0.564 ± 0.051 (20.2 ± 1.0)	0.640 ± 0.007 (5.7 ± 0.1)	0.602
Chronos-Bolt-tiny	0.525 ± 0.015 (21.6 ± 0.3)	0.621 ± 0.017 (6.0 ± 0.1)	0.573
SimMTM	0.642 ± 0.028 (18.8 ± 0.7)	0.687 ± 0.018 (5.3 ± 0.1)	0.665
T-BERT (ours)	0.660 ± 0.041 (18.3 ± 1.0)	0.693 ± 0.011 (5.3 ± 0.1)	0.677
VITA-Std. Normal (ours)	0.706 ± 0.025 (17.1 ± 0.7)	0.698 ± 0.020 (5.2 ± 0.2)	0.702
VITA-Sinusoidal (ours)	0.729 ± 0.008 (16.3 ± 0.2)	0.722 ± 0.005 (5.0 ± 0.1)	0.726

Table 1: Performance on the 5 most extreme years. Results averaged across 3 random seeds (1234, 5678, 2025) and best results **bolded**. The OLS baseline shows no change since it is deterministic.

using hyperparameters optimized for extreme years. We test both 15-year and 30-year training periods to assess data efficiency requirements.

Forward Gap Robustness

We also evaluate forward gap robustness across five experiments with 5-year gaps: train on 1994–2009/test on 2014, train on 1995–2010/test on 2015, and so forth through 2018.

Ablation Studies

We ablate: (1) pretraining vs. random initialization, (2) variational vs. MSE objective, (3) sinusoidal vs. normal priors, and (4) spatial generalization by pretraining on weather grids excluding continental USA, focusing on extreme weather performance.

All pretraining experiments run on four L40S GPUs and all finetuning experiments run on one L40S GPU with identical computational budgets across methods. The code, pre-trained models, and datasets will be publicly released upon publication to facilitate reproducibility and broader agricultural AI research.

Results

Extreme Year Performance

VITA-Sinusoidal achieves 0.729 ± 0.008 R^2 for corn and 0.722 ± 0.005 R^2 for soybean on the five most extreme weather years (Table 1), representing +10.5% and +4.2% improvements over T-BERT (0.660 and 0.693 respectively). These gains translate to 2.0 bu/ac corn and 0.3 bu/ac soybean RMSE reductions over T-BERT—critically important during droughts like 2012 when accurate forecasts inform billions in crop insurance decisions. The remarkably low variance across random seeds demonstrates the approach’s stability.

Figure 4 reveals VITA outperforms T-BERT on 8/10 individual extreme years and surpasses both SimMTM and Chronos-Bolt on 9/10 evaluations (paired t-test across 30 instances from 3 seeds, $p < 0.0001$). The rare underperformances occur when baselines already achieve high accuracy (soybean 2012: 0.689 R^2 , 2016: 0.834 R^2), leaving minimal room for improvement. Notably, Chronos-Bolt—despite being 4.5× larger (9M vs 2M parameters) and pretrained 890k

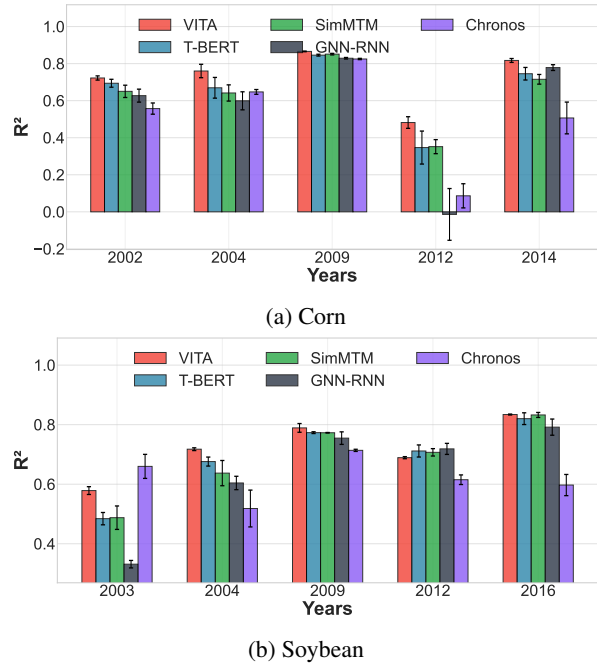


Figure 4: Individual R^2 comparisons on extreme years showing consistent improvements of VITA-Sinusoidal over other baselines.

sequences (Ansari et al. 2024)—struggles due to the data asymmetry problem.

We also note that the traditional methods fail catastrophically (OLS: 0.227 corn R^2 , XGBoost: 0.135 R^2 with soil data) during extreme years, while soil-enriched deep learning shows moderate success (GNN-RNN: 0.564 corn, CNN-RNN: 0.256). Among transformer models, pretraining strategy determines success—SimMTM’s temporal masking (0.642 corn) and Chronos’s general-purpose variational pretraining. Comparing T-BERT (0.660) to VITA-Std Normal (0.706) and VITA-Sinusoidal (0.729), we observe that, variational objectives provide +7% improvement, with sinusoidal priors adding another +3% by capturing seasonal structure.

Method	Corn 15yr R ² (RMSE)	Corn 30yr R ² (RMSE)	Soybean 15yr R ² (RMSE)	Soybean 30yr R ² (RMSE)
OLS	0.515 (24.5)	0.508 (24.1)	0.673 (6.0)	0.660 (6.1)
XGBoost	0.439 (27.4)	0.310 (29.2)	0.602 (6.5)	0.564 (7.1)
CNN-RNN	0.659 (20.7)	0.635 (20.8)	0.721 (5.6)	0.671 (6.0)
GNN-RNN	0.788 (16.6)	0.785 (16.5)	0.800 (4.7)	0.810 (4.6)
Chronos-Bolt-tiny	0.704 (19.5)	0.693 (19.7)	0.704 (5.7)	0.724 (5.6)
SimMTM	0.753 (17.9)	0.768 (17.2)	0.814 (4.6)	0.822 (4.5)
T-BERT (ours)	0.791 (16.5)	0.780 (16.8)	0.831 (4.4)	0.837 (4.3)
VITA-Sinusoidal (ours)	0.827 (16.0)	0.837 (15.5)	0.833 (4.3)	0.837 (4.2)

Table 2: Standard years (2014-2018) performance. Best results **bolded**.

Crop	Model	Full R ² (RMSE)	Week 30 R ² (RMSE)
Corn	OLS	0.227 (27.7)	0.227 (27.7)
	SimMTM	0.642 (18.8)	0.568 (20.5)
	T-BERT	0.660 (18.3)	0.589 (20.2)
	VITA-Std. Norm.	0.706 (17.1)	0.642 (18.9)
	VITA-Sinusoidal	0.729 (16.3)	0.689 (17.6)
Soybean	OLS	0.460 (7.0)	0.382 (7.5)
	SimMTM	0.687 (5.3)	0.481 (6.8)
	T-BERT	0.693 (5.3)	0.508 (6.7)
	VITA-Std. Norm.	0.698 (5.2)	0.551 (6.3)
	VITA-Sinusoidal	0.722 (5.0)	0.560 (6.2)

Table 3: Early-season forecasting on extreme years. Full: 7 years weather through end of season (52 weeks). Week 30: cutoff at end of July (30 weeks of final year).

Operational viability is confirmed through two stress tests. Weather cut off at July (week 30 of final year) VITA-Sinusoidal maintains strong performance, achieving 0.689 R² on corn and 0.560 R² – nearly 3.0× and 1.5× better than OLS baselines, respectively (Table 3). The performance drop for soybean is particularly sharp across all models, as its late pod-filling stage makes yields highly sensitive to August rainfall and temperature stress. (Westcott and Jewison 2013)

Lastly, we note that the XGBoost model underperforms in all instances due to correlated weather features, and will require feature engineering to get competitive performance.

Reduced temporal context (5 years vs 7 years) shows VITA-Sinusoidal achieves 0.697 R² corn and 0.684 R² soybean, outperforming most baselines despite using 28% less data (Appendix 4).

Standard Years and Forward Gap Robustness

Standard years (2014-2018) validate that extreme-weather optimization doesn’t compromise normal conditions. VITA achieves 0.827 R² for corn and 0.833 R² for soybean with 15-year training—improvements of +4.6% and +0.2% over T-BERT respectively. The contrast with extreme years (+10.5% corn improvement) supports our core hypothesis: variational uncertainty modeling provides greatest value

precisely when predictions are hardest. With 30-year training, corn performance rises to 0.837 R² (+7.3% over T-BERT), suggesting additional historical data helps but yields diminishing returns compared to better representations.

Five-year temporal shift (training on 1994-2009, testing on 2014-2018) stresses whether learned patterns generalize beyond training conditions or merely memorize era-specific correlations. VITA achieves 0.797 R² corn and 0.819 R² soybean—maintaining the +1.9% and +2.0% margins over T-BERT seen in standard evaluation. Meanwhile, the CNN-RNN and GNN-RNN models suffer noticeable degradation (0.718 corn, down from 0.788), revealing their soil-enhanced features do not help with temporal robustness.

Ablation Studies

Pretraining and Spatial Transfer

Pretraining is critical for VITA’s performance. Without pretraining, both VITA variants show high variance across hyperparameters (± 0.23 corn R², ± 0.14 soybean R²) and achieve only 0.47 and 0.57 mean R² respectively (Table 5). Pretraining on Central and South American weather—excluding all US continental data—provides substantial improvements of +34-37% corn and +17-19% soybean ($t = 3.61 - 3.82, p < 0.01$), demonstrating that VITA learns universal weather-agriculture relationships rather than region-specific patterns.

Full Americas pretraining (including US weather outside Corn Belt counties and target years) further improves performance to approximately 0.70 R² for both crops with continued low variance (± 0.015 -0.019). The +50% corn and +22% soybean improvements over no pretraining ($t = 5.35 - 5.49, p < 0.001$) highlight that variational objectives are particularly initialization-sensitive—they either converge to strong solutions with pretrained weights or fail to escape poor local minima without them. For comparison, T-BERT shows smaller but still significant pretraining gains (+10.8% corn, +5.0% soybean, $t = 9.13, p < 0.001$) with consistently lower variance across all conditions, as detailed in Appendix 4.

Discussion

VITA-Sinusoidal achieves statistically significant improvements over architecturally identical T-BERT baselines ($p <$

Method	Corn	Soybean	Mean R ²
	R ² (RMSE)	R ² (RMSE)	
OLS	0.471 (25.6)	0.634 (6.4)	0.552
XGBoost	0.159 (34.4)	0.433 (8.2)	0.296
CNN-RNN	0.556 (23.9)	0.659 (6.2)	0.608
GNN-RNN	0.718 (18.9)	0.785 (4.9)	0.752
Chronos-Bolt-tiny	0.631 (21.7)	0.685 (5.9)	0.658
SimMTM	0.705 (19.7)	0.776 (5.0)	0.741
T-BERT (ours)	0.782 (16.9)	0.803 (4.7)	0.793
VITA-Sinusoidal (ours)	0.797 (16.3)	0.819 (4.5)	0.808

Table 4: Forward gap robustness: 5-year temporal shift (train: 1994-2009, test: 2014-2018). Best results **bolded**.

Prior	Pretraining	Corn R ²	Soybean R ²	t-stat / p-value
Std. Normal	None	0.463 ± 0.230	0.575 ± 0.134	-
	Non-US	0.632 ± 0.018	0.674 ± 0.020	3.82 / 7.5 × 10 ⁻⁴
	Full	0.706 ± 0.015	0.698 ± 0.017	5.49 / 9.3 × 10 ⁻⁶
Sinusoidal	None	0.469 ± 0.227	0.569 ± 0.139	-
	Non-US	0.627 ± 0.020	0.669 ± 0.021	3.61 / 1.3 × 10 ⁻³
	Full	0.703 ± 0.015	0.698 ± 0.019	5.35 / 1.3 × 10 ⁻⁵

Table 5: VITA pretraining ablation across 27 hyperparameter (random seed 1234).

0.0001), with gains most pronounced during extreme weather when accurate predictions are most critical. This superior performance stems from rich latent representations that avoid the collapse seen in T-BERT (15.7% vs. 84.0% variance in top two PCA components; Figure 5), enabling better differentiation between normal and extreme conditions. VITA exceeds GNN-RNN despite lacking soil data, demonstrating that historical yields can proxy soil characteristics when paired with rich weather representations.

Operational Context and Social Impact. Current USDA operational forecasts—including ERS regression models (Westcott and Jewison 2013) and NASS survey-driven approaches (NASS 2023)—rely on simpler models with hand-crafted features, achieving 0.227 R² for extreme corn years with our OLS baseline. VITA’s 3.2× improvement (0.729 R²) translates to substantial impact: 11.4 bu/ac RMSE reduction over OLS and 2.0 bu/ac over T-BERT across 88.7M Corn Belt acres (National Corn Growers Association 2024). At \$4.70/bushel (DTN Progressive Farmer 2025), this translates to \$4.75B and \$800M in value, respectively. This accuracy is critical for the Federal Crop Insurance Program managing billions in premiums (USDA Economic Research Service 2024) and for policy responses during droughts. Deployment requires minimal infrastructure (single GPU, 2.5 hours training) with only public data, enabling integration into existing agricultural statistics systems.

Spatial Transfer and Global Food Security. Pretraining on Central/South American weather—climatically distinct from the U.S. Corn Belt—significantly improves U.S. predictions ($t = 3.61$, $p < 0.01$; Table 5). This cross-continental transfer demonstrates that VITA learns universal

weather-agriculture relationships (temperature stress, precipitation deficits, radiation anomalies) rather than region-specific patterns. For global food security, models pretrained on data-rich regions can enhance predictions in data-scarce areas despite climatic differences.

Broader Applicability and Limitations. The decoder-free variational framework generalizes beyond agriculture to any setting with rich sensors at training and sparse sensors at inference (e.g., ICU vitals vs. labs, IoT vs. industrial telemetry). Current evaluation focuses on U.S. Corn Belt corn and soybean (Khaki, Wang, and Archontoulis 2019; Fan et al. 2021); extending to other crops and regions remains future work. We commit to open-sourcing implementation, preprocessing scripts, model weights, and documentation for new region adaptation. Data privacy concerns are negligible as we use aggregated public meteorological data, ensuring equitable access through transparency.

Conclusion

We introduced VITA, a variational pretraining framework for forecasting crop yield under extreme weather. By leveraging satellite weather datasets through decoder-free variational learning and seasonality-aware priors, VITA achieves state-of-the-art performance on extreme weather years (R² = 0.729 for corn, 0.727 for soybeans). The framework requires only basic weather variables available globally, allowing deployment in data-scarce regions where multi-modal approaches are infeasible. Our comprehensive evaluation across 763 US Corn Belt counties with statistical validation and spatial transfer experiments, demonstrates robust performance, and provides a scalable approach for AI-driven food security.

References

- Ansari, A. F.; Stella, L.; Turkmen, C.; Zhang, X.; Mercado, P.; Shen, H.; Shchur, O.; Rangapuram, S. S.; Arango, S. P.; Kapoor, S.; Zschiegner, J.; Maddix, D. C.; Wang, H.; Mahoney, M. W.; Torkkola, K.; Wilson, A. G.; Bohlke-Schneider, M.; and Wang, Y. 2024. Chronos: Learning the Language of Time Series. arXiv:2403.07815.
- Basir, M. S.; Chowdhury, M.; Islam, M. N.; and Ashik-E-Rabbani, M. 2021. Artificial neural network model in predicting yield of mechanically transplanted rice from transplanting parameters in Bangladesh. *Journal of Agriculture and Food Research*, 5: 100186.
- Beddington, J. 2010. Food security: contributions from science to a new and greener revolution. *Philosophical Transactions of the Royal Society B: Biological Sciences*, 365(1537): 61–71.
- Brown, O. L. I. 1951. The Clausius-Clapeyron equation. *Journal of Chemical Education*, 28(8): 428.
- Cao, Z.; Ma, Y.; and Zhang, Z. 2022. Corn Yield Prediction based on Remotely Sensed Variables Using Variational Autoencoder and Multiple Instance Regression. arXiv:2211.13286.
- Chen, T.; and Guestrin, C. 2016. XGBoost: A Scalable Tree Boosting System. In *Proceedings of the 22nd ACM SIGKDD International Conference on Knowledge Discovery and Data Mining*, KDD '16, 785–794. ACM.
- Chu, Z.; and Yu, J. 2020. An end-to-end model for rice yield prediction using deep learning fusion. *Computers and Electronics in Agriculture*, 174: 105471.
- Dong, J.; Wu, H.; Zhang, H.; Zhang, L.; Wang, J.; and Long, M. 2023. SimMTM: A Simple Pre-Training Framework for Masked Time-Series Modeling. arXiv:2302.00861.
- DTN Progressive Farmer. 2025. 2025 Spring Crop Insurance Price Discovery. Accessed: 2025-10-02.
- Fan, J.; Bai, J.; Li, Z.; Ortiz-Bobea, A.; and Gomes, C. P. 2021. A GNN-RNN Approach for Harnessing Geospatial and Temporal Information: Application to Crop Yield Prediction. *CoRR*, abs/2111.08900.
- Ferraz, M. A. J.; Barboza, T. O. C.; Piza, M. R.; Von Pinho, R. G.; and dos Santos, A. F. 2024. Sorghum grain yield estimation based on multispectral images and neural network in tropical environments. *Smart Agricultural Technology*, 9: 100661.
- Franceschi, J.-Y.; Dieuleveut, A.; and Jaggi, M. 2019. Un-supervised scalable representation learning for multivariate time series. In *Advances in Neural Information Processing Systems*, volume 32.
- Gandhi, N.; Petkar, O.; and Armstrong, L. J. 2016. Rice crop yield prediction using artificial neural networks. In *2016 IEEE Technological Innovations in ICT for Agriculture and Rural Development (TIAR)*, 105–110.
- Hasan, A.; Roozbehani, M.; and Dahleh, M. 2024. WeatherFormer: A Pretrained Encoder Model for Learning Robust Weather Representations from Small Datasets. arXiv:2405.17455.
- Hendrycks, D.; and Gimpel, K. 2017. Bridging Nonlinearities and Stochastic Regularizers with Gaussian Error Linear Units.
- Higgins, I.; Matthey, L.; Pal, A.; Burgess, C.; Glorot, X.; Botvinick, M.; Mohamed, S.; and Lerchner, A. 2017. beta-VAE: Learning Basic Visual Concepts with a Constrained Variational Framework. In *International Conference on Learning Representations*.
- Keating, B.; Carberry, P.; Hammer, G.; Probert, M.; Robertson, M.; Holzworth, D.; Huth, N.; Hargreaves, J.; Meinke, H.; Hochman, Z.; McLean, G.; Verburg, K.; Snow, V.; Dimes, J.; Silburn, M.; Wang, E.; Brown, S.; Bristow, K.; Asseng, S.; Chapman, S.; McCown, R.; Freebairn, D.; and Smith, C. 2003. An overview of APSIM, a model designed for farming systems simulation. *European Journal of Agronomy*, 18(3): 267–288. Modelling Cropping Systems: Science, Software and Applications.
- Khaki, S.; Wang, L.; and Archontoulis, S. V. 2019. A CNN-RNN Framework for Crop Yield Prediction. *Frontiers in Plant Science*, 10.
- Kingma, D. P.; Mohamed, S.; Jimenez Rezende, D.; and Welling, M. 2014. Semi-supervised learning with deep generative models. *Advances in neural information processing systems*, 27.
- Kingma, D. P.; and Welling, M. 2013. Auto-encoding variational bayes. *arXiv preprint arXiv:1312.6114*.
- Kwok, P. H.; and Qi, Q. 2021. A Variational U-Net for Weather Forecasting. *CoRR*, abs/2111.03476.
- Lin, F.; Guillot, K.; Crawford, S.; Zhang, Y.; Yuan, X.; and Tzeng, N.-F. 2024. An Open and Large-Scale Dataset for Multi-Modal Climate Change-aware Crop Yield Predictions. In *Proceedings of the 30th ACM SIGKDD Conference on Knowledge Discovery and Data Mining*, 5375–5386. ACM.
- Lobell, D. B.; Schlenker, W.; and Costa-Roberts, J. 2011. Climate trends and global crop production since 1980. *Science*, 333(6042): 616–620.
- McFarland, B. A.; AlKhalifah, N.; Bohn, M.; Bubert, J.; Buckler, E. S.; Ciampitti, I.; Edwards, J.; Ertl, D.; Gage, J. L.; Falcon, C. M.; Flint-Garcia, S.; Gore, M. A.; Graham, C.; Hirsch, C. N.; Holland, J. B.; Hood, E.; Hooker, D.; Jarquin, D.; Kaeppeler, S. M.; Knoll, J.; Kruger, G.; Lauter, N.; Lee, E. C.; Lima, D. C.; Lorenz, A.; Lynch, J. P.; McKay, J.; Miller, N. D.; Moose, S. P.; Murray, S. C.; Nelson, R.; Poudyal, C.; Rocheford, T.; Rodriguez, O.; Romay, M. C.; Schnable, J. C.; Schnable, P. S.; Scully, B.; Sekhon, R.; Silverstein, K.; Singh, M.; Smith, M.; Spalding, E. P.; Springer, N.; Thelen, K.; Thomison, P.; Tuinstra, M.; Wallace, J.; Walls, R.; Wills, D.; Wissler, R. J.; Xu, W.; Yeh, C. T.; and de Leon, N. 2020. Maize genomes to fields (G2F): 2014–2017 field seasons: genotype, phenotype, climatic, soil, and inbred ear image datasets. *BMC Research Notes*, 13(1): 71.
- Murray-Tortarolo, G. 2023. A breviary of Earth’s climate changes using Stephan-Boltzmann law. *Atmósfera*, 37.
- NASA. 2024. NASA Power API.

- NASS. 2023. The Yield Forecasting and Estimating Program of NASS. NASS Staff Report SEDMB 23-01, U.S. Department of Agriculture, Washington, D.C.
- National Corn Growers Association. 2024. Corn Production: USDA expects U.S. farmers to harvest about 88.7 million acres of corn for grain. Accessed: 2025-10-02.
- National Drought Mitigation Center; NOAA; and USDA. 2025. U.S. Drought Monitor. Accessed: 2025-07-31.
- Ndulue, E.; and Ranjan, R. S. 2021. Performance of the FAO Penman-Monteith equation under limiting conditions and fourteen reference evapotranspiration models in southern Manitoba. *Theoretical and Applied Climatology*, 143(3): 1285–1298.
- O. Tetens. 1930. Über einige meteorologische Begriffe (On some meteorological terms). *Z. Geophys.*, 6: 297–309.
- Oliveira, I.; Cunha, R. L. F.; Silva, B.; and Netto, M. A. S. 2018. A Scalable Machine Learning System for Pre-Season Agriculture Yield Forecast. arXiv:1806.09244.
- Palma, L.; Peraza, A.; Civantos, D.; Duarte, A.; Materia, S.; Ángel G. Muñoz; Peña-Izquierdo, J.; Romero, L.; Soret, A.; and Donat, M. G. 2025. Data-driven Seasonal Climate Predictions via Variational Inference and Transformers. arXiv:2503.20466.
- Razavi, M. A.; Nejadhashemi, A. P.; Majidi, B.; Razavi, H. S.; Kpodo, J.; Eeswaran, R.; Ciampitti, I.; and Prasad, P. V. 2024. Enhancing crop yield prediction in Senegal using advanced machine learning techniques and synthetic data. *Artificial Intelligence in Agriculture*, 14: 99–114.
- Sun, J.; Di, L.; Sun, Z.; Shen, Y.; and Lai, Z. 2019. County-Level Soybean Yield Prediction Using Deep CNN-LSTM Model. *Sensors*, 19(20): 4363.
- U.S. Census Bureau. 2025. Gazetteer Files: National Counties Gazetteer File. <https://www.census.gov/geographies/reference-files/time-series/geo/gazetteer-files.html>. County land and water area (ALAND_SQMI, AWATER_SQMI); median county land area can be computed from this file (author’s calculation). Page last revised 2025-09-10.
- U.S. Department of Agriculture, National Agricultural Statistics Service. 2023. Quick Stats Database. <https://quickstats.nass.usda.gov/>. Accessed: 2025-07-08.
- USDA Economic Research Service. 2024. Crop Insurance at a Glance. Accessed: 2025-10-02.
- USDA Farm Service Agency. 2019. Report: Farmers Prevented from Planting Crops on 19 Million Acres. <https://www.fsa.usda.gov/news-events/news/08-12-2019/report-farmers-prevented-planting-crops-19-million-acres>. Accessed: 2025-07-22.
- USDA National Agricultural Statistics Service. 2013. Crop Production 2012 Summary. https://www.nass.usda.gov/Newsroom/archive/2013/01_11_2013.php. Accessed: 2025-07-22.
- Vaswani, A.; Shazeer, N.; Parmar, N.; Uszkoreit, J.; Jones, L.; Gomez, A. N.; Kaiser, L.; and Polosukhin, I. 2017. Attention Is All You Need. arXiv:1706.03762.
- Wang, W.; Zhang, J.; Su, Q.; et al. 2024. Accurate initial field estimation for weather forecasting with a variational constrained neural network. *npj Climate and Atmospheric Science*, 7(1): 223.
- Westcott, P. C.; and Jewison, M. 2013. Weather Effects on Expected Corn and Soybean Yields. Technical Report FDS-13g-01, U.S. Department of Agriculture, Economic Research Service.
- Williams, B.; and Pounds-Barnett, G. 2024. As U.S. Farmers Respond to Crop Price Changes, Trends in Planted Acreage Emerge. *Amber Waves*.
- Woo, G.; Liu, C.; Sahoo, D.; Kumar, A.; and Hoi, S. 2022. CoST: Contrastive Learning of Disentangled Seasonal-Trend Representations for Time Series Forecasting. arXiv:2202.01575.
- Wu, H.; Xu, J.; Wang, J.; and Long, M. 2023. Patchst: A general-purpose patch-based transformer for time series forecasting. In *The Eleventh International Conference on Learning Representations*.
- Wu, X.; Xiao, X.; Steiner, J.; Yang, Z.; Qin, Y.; and Wang, J. 2021. Spatiotemporal Changes of Winter Wheat Planted and Harvested Areas, Photosynthesis and Grain Production in the Contiguous United States from 2008–2018. *Remote Sensing*, 13(9).
- You, J.; Li, X.; Low, M.; Lobell, D.; and Ermon, S. 2017. Deep Gaussian process for crop yield prediction based on remote sensing data. *arXiv preprint arXiv:1704.02720*.
- Yue, Z.; Wang, Y.; Pang, J.; Zhang, F.; Yang, W.; Sun, L.; Li, J.; Wang, J.; and Zhang, Y. 2022. Ts2vec: Towards universal representation of time series. In *Proceedings of the AAAI conference on artificial intelligence*, volume 36, 8980–8988.
- Zerveas, G.; Jayaraman, S.; Patel, D.; Bhamidipaty, A.; and Eickhoff, C. 2021. A transformer-based framework for multivariate time series representation learning. In *Proceedings of the 27th ACM SIGKDD conference on knowledge discovery & data mining*, 2114–2124.

Reproducibility Checklist

Instructions for Authors:

This document outlines key aspects for assessing reproducibility. Please provide your input by editing this `.tex` file directly.

For each question (that applies), replace the “Type your response here” text with your answer.

Example: If a question appears as

```
\question{Proofs of all novel claims
are included} {(yes/partial/no)}
Type your response here
```

you would change it to:

```
\question{Proofs of all novel claims
are included} {(yes/partial/no)}
yes
```

Please make sure to:

- Replace ONLY the “Type your response here” text and nothing else.

- Use one of the options listed for that question (e.g., **yes**, **no**, **partial**, or **NA**).
- **Not** modify any other part of the `\question` command or any other lines in this document.

You can `\input` this `.tex` file right before `\end{document}` of your main file or compile it as a stand-alone document. Check the instructions on your conference’s website to see if you will be asked to provide this checklist with your paper or separately.

1. General Paper Structure

- 1.1. Includes a conceptual outline and/or pseudocode description of AI methods introduced (yes/partial/no/NA) **Yes**
- 1.2. Clearly delineates statements that are opinions, hypothesis, and speculation from objective facts and results (yes/no) **Yes**
- 1.3. Provides well-marked pedagogical references for less-familiar readers to gain background necessary to replicate the paper (yes/no) **Yes**

2. Theoretical Contributions

- 2.1. Does this paper make theoretical contributions? (yes/no) **Yes**

If yes, please address the following points:

- 2.2. All assumptions and restrictions are stated clearly and formally (yes/partial/no) **Yes**
- 2.3. All novel claims are stated formally (e.g., in theorem statements) (yes/partial/no) **Yes**
- 2.4. Proofs of all novel claims are included (yes/partial/no) **Yes**
- 2.5. Proof sketches or intuitions are given for complex and/or novel results (yes/partial/no) **Yes**
- 2.6. Appropriate citations to theoretical tools used are given (yes/partial/no) **Yes**
- 2.7. All theoretical claims are demonstrated empirically to hold (yes/partial/no/NA) **Yes**
- 2.8. All experimental code used to eliminate or disprove claims is included (yes/no/NA) **NA**

3. Dataset Usage

- 3.1. Does this paper rely on one or more datasets? (yes/no) **Yes**

If yes, please address the following points:

- 3.2. A motivation is given for why the experi-

ments are conducted on the selected datasets (yes/partial/no/NA) **Yes**

- 3.3. All novel datasets introduced in this paper are included in a data appendix (yes/partial/no/NA) **Yes**
- 3.4. All novel datasets introduced in this paper will be made publicly available upon publication of the paper with a license that allows free usage for research purposes (yes/partial/no/NA) **Yes**
- 3.5. All datasets drawn from the existing literature (potentially including authors’ own previously published work) are accompanied by appropriate citations (yes/no/NA) **Yes**
- 3.6. All datasets drawn from the existing literature (potentially including authors’ own previously published work) are publicly available (yes/partial/no/NA) **Yes**
- 3.7. All datasets that are not publicly available are described in detail, with explanation why publicly available alternatives are not scientifically satisfying (yes/partial/no/NA) **NA**

4. Computational Experiments

- 4.1. Does this paper include computational experiments? (yes/no) **Yes**

If yes, please address the following points:

- 4.2. This paper states the number and range of values tried per (hyper-) parameter during development of the paper, along with the criterion used for selecting the final parameter setting (yes/partial/no/NA) **Yes**
- 4.3. Any code required for pre-processing data is included in the appendix (yes/partial/no) **Yes**
- 4.4. All source code required for conducting and analyzing the experiments is included in a code appendix (yes/partial/no) **Yes**
- 4.5. All source code required for conducting and analyzing the experiments will be made publicly available upon publication of the paper with a license that allows free usage for research purposes (yes/partial/no) **Yes**
- 4.6. All source code implementing new methods have comments detailing the implementation, with references to the paper where each step comes from (yes/partial/no) **Yes**
- 4.7. If an algorithm depends on randomness, then the method used for setting seeds is described in a way sufficient to allow replication of results (yes/partial/no/NA) **Yes**
- 4.8. This paper specifies the computing infrastructure used for running experiments (hardware and

software), including GPU/CPU models; amount of memory; operating system; names and versions of relevant software libraries and frameworks (yes/partial/no) **Yes**

- 4.9. This paper formally describes evaluation metrics used and explains the motivation for choosing these metrics (yes/partial/no) **Yes**
- 4.10. This paper states the number of algorithm runs used to compute each reported result (yes/no) **Yes**
- 4.11. Analysis of experiments goes beyond single-dimensional summaries of performance (e.g., average; median) to include measures of variation, confidence, or other distributional information (yes/no) **Yes**
- 4.12. The significance of any improvement or decrease in performance is judged using appropriate statistical tests (e.g., Wilcoxon signed-rank) (yes/partial/no) **Yes**
- 4.13. This paper lists all final (hyper-)parameters used for each model/algorithm in the paper’s experiments (yes/partial/no/NA) **Yes**

Appendix

Mathematical Framework

We define $z \in \mathbb{R}^{364 \times 31}$ as the full set of meteorological variables available during pretraining—such as radiation fluxes, humidity, wind speed, and surface pressure—which together describe the latent physical state of the atmosphere over 364-week sequences (7 years of weekly means). The observed variables $x \in \mathbb{R}^{364 \times 6}$ are a subset of basic weather statistics used in downstream tasks, including quantities like precipitation, and min/max temperature. For brevity, in the following mathematical derivations, we use $d_z = 364 \times 31$ and $d_x = 364 \times 6$ to represent the flattened dimensions. We have two datasets: (1) A large pretraining weather dataset $\mathcal{D}_w = \{(x_i, z_i)\}_{i=1}^{N_w}$ where both basic weather variables x_i and detailed weather states z_i are observed, and (2) A crop yield dataset $\mathcal{D}_y = \{(x_j, y_j)\}_{j=1}^{N_y}$ where only basic weather variables x_j and yield targets y_j are observed, but detailed weather states z_j remain unobserved. Our goal is to predict crop yield y_j given basic weather variables x_j by learning the detailed weather representation z_j during the pretraining phase. Figure 2 shows a graphical model of the setup.

A key insight of our framework is the structured relationship between the detailed meteorological state z (e.g., radiation fluxes, humidity) and the basic weather statistics x (e.g., temperature, vapor pressure) used for the downstream task. Many variables in x can be closely approximated or deterministically computed from components in z via our deterministic-decoder assumption.

Inspired by this, we adopt the structural modeling assumption that $p_\theta(x | z) \approx 1$ for valid pairs. While not strictly true for all possible weather variables, this is a

meteorologically-grounded modeling assumption that is reasonable for our dataset. This assumption allows us to eliminate the decoder term in the variational objective.

Pretraining Objective During pretraining, paired observations $(x_i, z_i) \in \mathcal{D}_w$ can be directly used to fit the likelihood function of $q_\phi(z_i | x_i)$. However, naively fitting likelihood leads to posterior collapse and an overconfident encoder. We therefore employ β -VAE style objective (Higgins et al. 2017) that balances reconstruction fidelity with regularization:

$$\mathcal{L}_{\text{pretrain}} = -\mathbb{E}_{(x_i, z_i) \sim \mathcal{D}_w} \left[\log q_\phi(z_i | x_i) + \alpha \text{KL}[q_\phi(z_i | x_i) \| p_\theta(z_i)] \right] \quad (9)$$

where $\alpha > 0$ controls regularization strength. The first term encourages accurate prediction of observed detailed weather states, while the KL term prevents posterior collapse and trains the prior parameters θ .

Fine-tuning Objective Next we derive the variational lower bound for the crop yield prediction. For each sample $(x_j, y_j) \in \mathcal{D}_y$, the log-likelihood is:

$$\log p_\theta(y_j | x_j) = \log \int p_\theta(y_j | z_j) p_\theta(z_j | x_j) dz_j \quad (10)$$

Applying Jensen’s inequality with variational distribution $q_\phi(z_j | x_j)$:

$$\log p_\theta(y_j | x_j) \geq \mathbb{E}_{q_\phi(z_j | x_j)} [\log p_\theta(y_j | z_j)] - \text{KL}[q_\phi(z_j | x_j) \| p_\theta(z_j | x_j)] \quad (11)$$

Using Bayes’ rule: $p_\theta(z_j | x_j) = \frac{p_\theta(x_j | z_j) p_\theta(z_j)}{p_\theta(x_j)}$ on the KL-Divergence and ignoring constants, we derive the standard semi-supervised VAE objective (Kingma et al. 2014):

$$\log p_\theta(y_j | x_j) \geq \mathbb{E}_{q_\phi(z_j | x_j)} [\log p_\theta(y_j | z_j)] + \mathbb{E}_{q_\phi(z_j | x_j)} [\log p_\theta(x_j | z_j)] - \text{KL}[q_\phi(z_j | x_j) \| p_\theta(z_j)] \quad (12)$$

Since by assumption, the detailed weather state z_j deterministically generates basic weather statistics x_j , we have $p_\theta(x_j | z_j) = 1$ for valid pairs. This eliminates the decoder term $\mathbb{E}_{q_\phi(z_j | x_j)} [\log p_\theta(x_j | z_j)]$, yielding:

$$\mathcal{L}_{\text{yield}} = -\mathbb{E}_{q_\phi(z_j | x_j)} [\log p_\theta(y_j | z_j)] + \text{KL}[q_\phi(z_j | x_j) \| p_\theta(z_j)] \quad (13)$$

This loss is computed by first sampling $z_j \sim q_\phi(z_j | x_j)$ with the reparameterization trick (Kingma and Welling 2013) and passed to the yield head for yield prediction.

Distributional Assumptions and Prior Choices We assume the variational posterior $q_\phi(z | x)$ to be a diagonal Gaussian whose parameters are predicted by a transformer encoder:

$$q_\phi(z | x) = \mathcal{N}(z; \mu_\phi(x), \text{diag}(\sigma_\phi^2(x))) \quad (14)$$

The choice of prior $p_\theta(z)$ depends on the task structure. While standard VAEs (Kingma and Welling 2013; Kingma et al. 2014) use unit normal priors, weather data exhibits temporal patterns that motivate more sophisticated choices.

Standard Gaussian Prior. The simplest choice is $p_\theta(z) = \mathcal{N}(0, I)$.

Sinusoidal Prior. To capture seasonal patterns:

$$p_\theta(z) = \mathcal{N}(\mu_{\text{sin}}, \text{diag}(\sigma_{\text{sin}}^2)) \quad (15)$$

$$\mu_{\text{sin},k} = A_k \sin(\theta_k \cdot \text{pos} + \theta_{0,k}) \quad (16)$$

where parameters A_k , θ_k , $\theta_{0,k}$, and $\sigma_{\text{sin},k}^2$ are learned during pretraining for each dimension k .

Gaussian Mixture Prior. While not explored in this paper, a sophisticated prior to capture more complex temporal weather patterns for other fine-tuning tasks could be:

$$p_\theta(z) = \sum_{j=1}^K w_j \mathcal{N}(\mu_{j,\text{sin}}, \text{diag}(\sigma_{j,\text{sin}}^2)) \quad (17)$$

In this case, the KL term in the loss has no closed form formula and will require Monte Carlo sampling via the reparameterization trick.

Yield Distribution. Crop yield depends not only on the current year’s weather representation z_j but also on historical yield patterns $y_{\text{past},j}$ that capture local soil conditions, management practices, and cultivar effects. For continuous yield targets y_j , we assume:

$$p_\theta(y_j | z_j) = \mathcal{N}(y_j; \mu_\theta(z_j, y_{\text{past},j}), \sigma_y^2) \quad (18)$$

where $\mu_\theta(z_j, y_{\text{past},j})$ is the mean yield predicted by a neural network with parameters θ , and σ_y^2 is a noise hyperparameter.

Practical Fine-tuning Objective Substituting the yield likelihood (Equation (18)) into the variational lower bound (Equation (13)):

$$\begin{aligned} \mathcal{L}_{\text{yield}} &= -\mathbb{E}_{q_\phi(z_j | x_j)} [\log p_\theta(y_j | z_j)] \\ &\quad + \text{KL}[q_\phi(z_j | x_j) \| p_\theta(z_j)] \\ &= \mathbb{E}_{q_\phi(z_j | x_j)} \left[\frac{1}{2\sigma_y^2} (y_j - \mu_\theta(z_j, y_{\text{past},j}))^2 \right] \\ &\quad + \text{KL}[q_\phi(z_j | x_j) \| p_\theta(z_j)] + C \end{aligned} \quad (19)$$

where C is a constant. Dropping constants and absorbing $\frac{1}{2\sigma_y^2}$ into the hyperparameter β :

$$\mathcal{L}_{\text{yield}} = \|y_j - \hat{y}_j\|^2 + \beta \cdot \text{KL}[q_\phi(z_j | x_j) \| p_\theta(z_j)] \quad (20)$$

where $\hat{y}_j = \mathbb{E}_{q_\phi(z_j | x_j)} [\mu_\theta(z_j, y_{\text{past},j})]$ is the predicted yield. Note that Equation (20) is still the variational lower bound and the β multiplier does not originate from the weakening of the variational objective.

KL Divergence Computation For practical implementation, we need to compute the KL divergence term $\text{KL}[q_\phi(z_j | x_j) \| p_\theta(z_j)]$ in both the pretraining and fine-tuning objectives. If both distributions are diagonal Gaussians, this has a closed form.

Standard Gaussian Prior. When $p_\theta(z) = \mathcal{N}(0, I)$ and $q_\phi(z | x) = \mathcal{N}(\mu_\phi(x), \text{diag}(\sigma_\phi^2(x)))$:

$$\begin{aligned} \text{KL}[q_\phi(z | x) \| p_\theta(z)] &= \frac{1}{2} \sum_{k=1}^{d_z} \left[\sigma_{\phi,k}^2(x) + \mu_{\phi,k}^2(x) - 1 \right. \\ &\quad \left. - \log \sigma_{\phi,k}^2(x) \right] \end{aligned} \quad (21)$$

Sinusoidal Prior. When $p_\theta(z) = \mathcal{N}(\mu_{\text{sin}}, \text{diag}(\sigma_{\text{sin}}^2))$ with $\mu_{\text{sin},k} = A_k \sin(\theta_k \cdot \text{pos} + \theta_{0,k})$:

$$\begin{aligned} \text{KL}[q_\phi(z | x) \| p_\theta(z)] &= \frac{1}{2} \sum_{k=1}^{d_z} \left[\frac{\sigma_{\phi,k}^2(x)}{\sigma_{\text{sin},k}^2} \right. \\ &\quad + \frac{(\mu_{\phi,k}(x) - \mu_{\text{sin},k})^2}{\sigma_{\text{sin},k}^2} \\ &\quad \left. - 1 - \log \frac{\sigma_{\phi,k}^2(x)}{\sigma_{\text{sin},k}^2} \right] \end{aligned} \quad (22)$$

Gaussian Mixture Prior. For the mixture prior $p_\theta(z) = \sum_{j=1}^K w_j \mathcal{N}(\mu_{j,\text{sin}}, \text{diag}(\sigma_{j,\text{sin}}^2))$, the KL divergence has no closed form and requires Monte Carlo estimation:

$$\begin{aligned} \text{KL}[q_\phi(z | x) \| p_\theta(z)] &\approx \frac{1}{L} \sum_{l=1}^L \left[\log q_\phi(z^{(l)} | x) \right. \\ &\quad \left. - \log p_\theta(z^{(l)}) \right] \end{aligned} \quad (23)$$

where $z^{(l)} \sim q_\phi(z | x)$ are samples obtained via the reparameterization trick.

Latent Space Analysis To empirically validate how different prior choices affect the learned representations, we analyze the latent space structure using Principal Component Analysis (PCA) on two extreme years: 2004 (exceptionally good weather with record-breaking yield) and 2012 (record drought with exceptionally bad yield). Figure 5 visualizes these latent structures.

T-BERT, trained without a variational prior, shows a highly compressed latent space with 84.0% of total variance captured by just two principal components and minimal separation between years—indicating limited representational flexibility. The standard normal prior introduces posterior diversity and improves year-wise separation, but most variance remains concentrated along the x-axis (25.6%), suggesting over-regularization that forces the model to rely heavily on one latent direction. In contrast, the sinusoidal prior results in only 15.7% of variance explained by the top two components (14.0% and 1.7%), despite having tighter clustering. This indicates the sinusoidal model distributes information more evenly across the full latent space, yielding richer representations. These findings confirm that seasonality-aware priors enforce meaningful structure without excessive compression.

Experimental Setup and Implementation Details

This section provides comprehensive details on datasets, evaluation protocols, model configurations, and computational requirements to ensure full reproducibility.

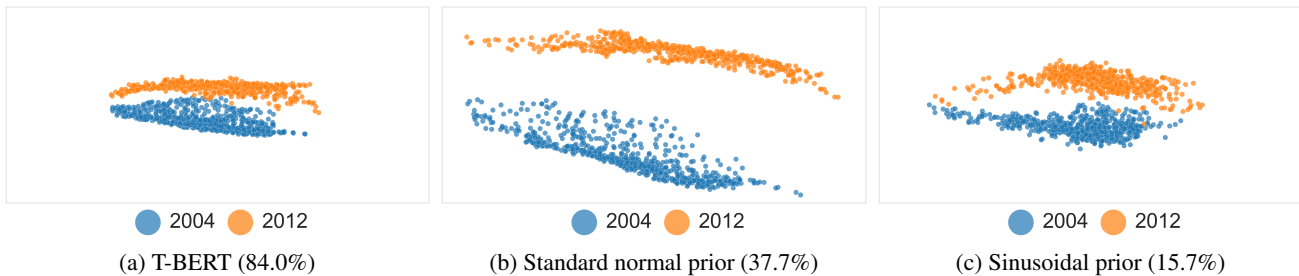


Figure 5: PCA visualization of the latent weather representations for two extreme years (2004: record-breaking yield, 2012: extreme drought) under different modeling choices. (a) T-BERT (non-variational) shows limited separation and explains 84.0% of variance in 2D, reflecting a narrow, collapsed latent space. (b) VITA with a standard normal prior yields more separated clusters and explains 34.7% of variance. (c) Sinusoidal prior induces visually tighter clusters but with only 15.7% explained variance, indicating even spread of variance into higher-order components.

Dataset Spatial Coverage

Locations. Our approach leverages two distinct spatial datasets with different coverage and resolution. The pre-training dataset contains 116 spatial grids at 0.5° resolution covering the continental United States, Central America and South America, with 108 grids used for training and 8 grids for validation. The fine-tuning dataset focuses on 763 counties within the US Corn Belt region, representing the core agricultural areas for corn and soybean production. Figure 7 illustrates the spatial coverage of both datasets, demonstrating how weather knowledge learned from the broader Americas region transfers effectively to US agricultural counties.

Pretraining Dataset Variables. Table 14 shows a list of 31 weather measurements in the pretraining data. The first 28 measurements were downloaded from the NASA Power Project (NASA 2024) from 1984 to 2022. The last three were predicted using Tetens equation (Vapor Pressure and Vapor Pressure Deficit) and FAO-Penman-Monteith equation (Reference Evapotranspiration). The data was downloaded for daily measurements and weekly mean was computed for each variable.

Extreme Years Selection and Evaluation Protocol To rigorously evaluate model performance on unprecedented weather conditions, we identify extreme years using standardized deviations from historical norms. Table 6 presents our selection methodology: years are ranked by absolute z-score from their 5-year rolling mean yield, with the top 5 years per crop selected for evaluation. This captures both exceptionally favorable years (e.g., corn 2004 with +21.42% yield, z-score 5.25) and severe stress years (e.g., the 2012 drought with -27.15% corn yield, z-score 4.08).

Strict Hold-Out Protocol. For each extreme test year t_{test} , we train exclusively on the 15 preceding years $[t_{\text{test}} - 15, t_{\text{test}} - 1]$ and evaluate only on t_{test} . Training generates overlapping 7-year sequences with target years in $[t_{\text{test}} - 9, t_{\text{test}} - 1]$, ensuring t_{test} never appears during training. For example, when evaluating corn 2002, we train on 1987-2001 generating sequences (1987-1993) \rightarrow 1993, ..., (1995-2001) \rightarrow 2001, while (1996-2002) \rightarrow 2002 is only used for final evaluation.

Training Configuration Details

Pretraining Configuration. We pretrain on weather sequences using batch size 256, learning rate 5×10^{-4} , and maximum context length of 364 weeks (7 years). Progressive masking increases from 10 to 25 features over 100 epochs, with 10-epoch linear warmup followed by exponential decay ($\delta = 0.99$). The variational objective uses $\alpha = 0.5$ to balance reconstruction and KL regularization.

Fine-tuning Configuration. Following a similar setup to Khaki, Wang, and Archontoulis (2019) and Fan et al. (2021), we construct overlapping 7-year sequences ($t - 6, \dots, t$) for each county, generating 9 sequences from 15-year training windows. Each sequence predicts yield for year t using weather from all 7 years plus historical yields from $t - 6$ to $t - 1$. Training proceeds for 40 epochs with 10-epoch linear warmup and cosine annealing, selecting the best validation RMSE. We use 15-year windows for extreme year and robustness experiments, and test both 15-year and 30-year windows for standard years, with strict isolation between test runs to prevent data leakage.

Random Seeds. All experiments, unless noted otherwise, share random seed 1234. The best extreme year results were additionally validated across 3 seeds (1234, 5678, 2025) and averaged for robustness.

VITA Architecture Details Table 7 details the VITA architecture. The core transformer encoder uses 4 layers with 10 attention heads, hidden dimension $d_h = 200$, and MLP dimension $d_{\text{mlp}} = 800$, processing 364-week sequences. The weather output projection produces mean and variance (31×2) for the variational posterior. Weather attention aggregates 31 feature dimensions using a learned attention mechanism (hidden dim 16). The sinusoidal prior parameterizes amplitude, frequency, phase, and variance for 31 weather variables across 364 time positions (124×364 total parameters). All MLPs use GELU activation (Hendrycks and Gimpel 2017).

Computational Efficiency Table 8 presents runtime comparisons demonstrating that VITA’s variational objective adds minimal computational overhead. Fine-tuning requires

Crop	Year	Yield (Bu/Acre)	5-Year Mean	Deviation %	Abs. Z-Score
Corn	2004	153.25	126.21	21.42	5.25
	2012	107.55	147.64	27.15	4.08
	2009	162.09	144.78	11.96	2.21
	2002	118.71	126.32	6.03	1.58
	2014	170.83	140.52	21.58	1.45
Soybean	2009	46.01	42.57	8.07	4.72
	2003	32.63	38.22	14.63	3.81
	2012	38.10	43.41	12.24	2.78
	2004	42.44	36.75	15.48	2.23
	2016	54.88	44.67	22.85	2.09

Table 6: Top 5 extreme years selection based on yield deviation from 5-year rolling mean.

Component	Input	Hidden	Output
Weather Input Proj.	34	-	200
Transformer ($\times 4$)	200	800	200
Weather Output Proj.	200	-	31×2
Weather Attention	31	16	1
Yield MLP	36	120	1
Sine Prior Param.	-	-	124×364

Table 7: VITA Model Architecture

25.53 minutes per configuration—only 3.4% slower than non-variational T-BERT (24.69 min) while delivering statistically significant performance gains. SimMTM requires more pretraining time (32.56 min vs 27-29 min) due to its sophisticated temporal masking strategy, whereas VITA and T-BERT employ simpler feature-wise masking.

Method	Pretraining 4 \times L40S	Fine-tuning 1 \times L40S
OLS	N/A	6.4 ± 1.3 min
XGBoost	N/A	18.7 ± 1.4 min
CNN-RNN	N/A	8.58 ± 0.04 min
GNN-RNN	N/A	7.13 ± 0.03 min
Chronos-Bolt-tiny	N/A	44.7 ± 1.3 min
SimMTM	32.56 min	25.92 ± 0.01 min
T-BERT	27.42 min	24.69 ± 0.13 min
VITA-Sinusoidal	29.21 min	25.53 ± 0.58 min

Table 8: Runtime comparison on 4 \times L40S GPUs (pretraining) and 1 \times L40S GPU (fine-tuning).

Pretraining on 4 \times L40S GPUs takes 27-29 minutes, extrapolating to 108-116 minutes on a single L40S. Combined with 25-minute fine-tuning, the complete pipeline requires 133-141 minutes (≈ 2.5 hours) on a single GPU. The full hyperparameter grid search (27 configurations \times 2 crops = 54 experiments) totals 22.5-23.4 hours of fine-tuning time.

Complete Experimental Results and Analysis

Impact of Pretraining Across Hyperparameter Configurations Tables 9 and 10 comprehensively evaluate pretraining benefits across hyperparameter configurations (seed 1234). T-BERT shows consistent but moderate gains: +10.8% mean corn R^2 (0.647 vs 0.584, $t = 9.13$, $p < 0.001$) and +5.0% soybean R^2 (0.693 vs 0.660, $t = 4.36$, $p < 0.01$), with low variance (± 0.014 - 0.020) indicating stable, initialization-insensitive optimization.

In contrast, VITA variants exhibit dramatic improvements. Without pretraining, both VITA-Std. Normal and VITA-Sinusoidal show extremely high variance (± 0.227 - 0.230), indicating unstable optimization. Pretraining reduces variance by over 10 \times while boosting mean R^2 by +49-52% for corn and +21-23% for soybean (all $p < 0.001$), demonstrating that variational objectives critically depend on well-initialized priors.

Cross-Continental Transfer. Table 10 validates spatial generalization by pretraining exclusively on Central/South American weather (excluding all continental US data). Despite zero geographic overlap, pretraining still provides substantial gains: +33-37% corn R^2 and +17-19% soybean R^2 ($t = 3.61 - 3.82$, $p < 0.01$). This confirms VITA learns universal weather-agriculture relationships (e.g., temperature stress effects on photosynthesis) rather than location-specific patterns—critical for deployment in data-scarce regions.

Hyperparameter Robustness Analysis Figure 6 visualizes performance across 27 deep learning configurations: learning rates $\{2.5 \times 10^{-4}, 5 \times 10^{-4}, 1 \times 10^{-3}\} \times$ batch sizes $\{16, 32, 64\} \times$ regularization $\beta \in \{0, 10^{-4}, 10^{-3}\}$. XGBoost uses an equivalent 27-configuration search over estimators $\{100, 500, 1000\} \times$ depth $\{4, 6, 8\} \times$ learning rate $\{0.03, 0.05, 0.1\}$.

VITA-Sinusoidal consistently outperforms T-BERT across *all* configurations, with R^2 improvements ranging from +0.01 to +0.15. This systematic advantage across diverse hyperparameter settings demonstrates that performance gains are intrinsic to the variational framework rather than artifacts of hyperparameter tuning.

Statistical Significance Analysis Table 11 presents complete R^2 scores across extreme years and crops, enabling rig-

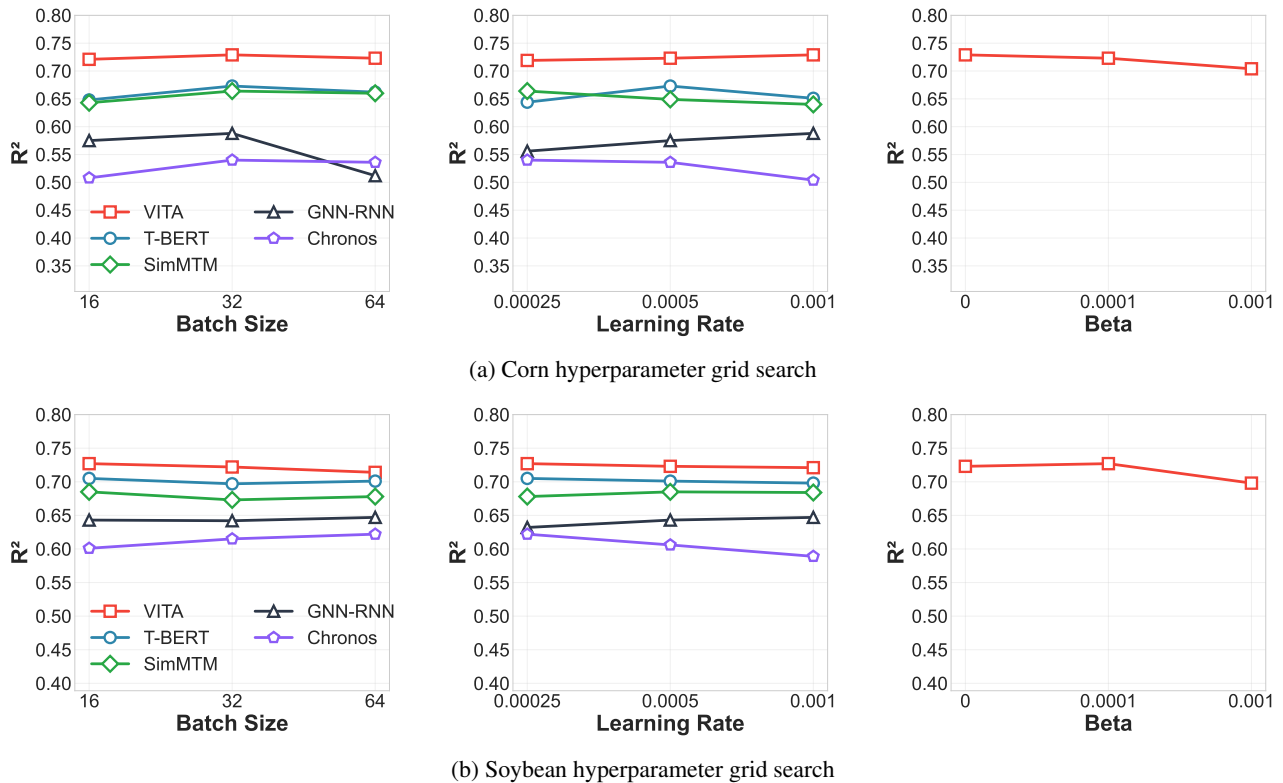


Figure 6: Hyperparameter robustness on extreme years: VITA-Sinusoidal consistently outperforms other baselines across all configurations tested. The CNN-RNN performs considerably worse and not shown in the plot.

orous statistical evaluation. We conduct both parametric and non-parametric tests on 30 paired comparisons (2 crops \times 5 extreme years \times 3 random seeds). Paired t-test: $t = 4.91$, $p < 0.0001$. Wilcoxon Signed-Rank Test: $W = 37.0$, $p < 0.0001$. VITA-Sinusoidal outperforms T-BERT in 25 of 30 comparisons, with mean R^2 improvement from 0.677 to 0.726 (+7.2% relative). Both tests confirm highly significant improvements.

Year-Permutation Ablation Study To rule out year-specific memorization, we conduct an ablation where calendar-year labels in the pretraining dataset (1984-2022) are randomly permuted while keeping weather measurements unchanged. This destroys temporal relationships, forcing the model to learn from weather statistics alone. Table 12 shows that pretraining still provides $\geq +0.03$ improvements with fixed hyperparameters, confirming benefits arise from weather representation learning rather than temporal memorization.

Critically, the sinusoidal prior shows reduced gains in the permuted setting (corn: +0.036 vs standard normal +0.047). This occurs because sinusoidal priors impose sine-wave structure to capture seasonality—when temporal order is randomized, this structure becomes counterproductive. This validates two key insights: (1) VITA’s pretraining learns robust weather patterns, not temporal correlations, and (2) the sinusoidal prior’s advantages require preserved temporal structure, confirming its role as a seasonality-aware regular-

izer.

Additional Baseline Experiments and Robustness Tests

Beyond the comprehensive ablations above, we evaluate VITA against domain-engineered baselines and stress-test performance under operational constraints (incomplete seasonal data, reduced temporal context).

OLS Baseline: Domain-Engineered Features To establish a domain-grounded comparison, we implement a linear regression baseline following the USDA Economic Research Service (ERS) yield modeling framework (Westcott and Jewison 2013). This approach uses agronomically-motivated features (temperature and precipitation during critical growth periods) conceptually similar to the NASS Yield Forecasting Program (NASS 2023), which relies on survey-based regression estimates.

The OLS model predicts yield as:

$$\hat{y}_t = \beta_0 + \beta_1 \cdot \text{Trend}_t + \beta_2 \cdot \bar{T}_{\text{crit}} + \beta_3 \cdot \bar{P}_{\text{crit}} + \beta_4 \cdot \bar{P}_{\text{crit}}^2 + \beta_5 \cdot S_{\text{June}} + \beta_6 \cdot \bar{y}_{\text{past}} \quad (24)$$

where $\text{Trend}_t = (t - 1970)/100$ captures technological progress, \bar{T}_{crit} and \bar{P}_{crit} represent mean temperature and precipitation during critical growth periods (July for corn weeks 26–30, July-August for soybean weeks 26–34), \bar{P}_{crit}^2 captures asymmetric moisture effects, S_{June} is June precipitation deficit, and \bar{y}_{past} is 5-year historical yield mean.

Crop	Model	Pretrained	Best R ²	Mean R ²	t-statistic	p-value
Corn	T-BERT	No	0.604	0.584 ± 0.015	9.13	1.7 × 10 ⁻⁵
		Yes	0.660	0.647 ± 0.014		
	VITA-Std	No	0.667	0.463 ± 0.230	5.49	9.3 × 10 ⁻⁶
		Yes	0.706	0.706 ± 0.015		
	VITA-Sinusoidal	No	0.672	0.469 ± 0.227	5.35	1.3 × 10 ⁻⁵
		Yes	0.729	0.703 ± 0.015		
Soybean	T-BERT	No	0.680	0.660 ± 0.020	4.36	2.4 × 10 ⁻³
		Yes	0.693	0.693 ± 0.012		
	VITA-Std	No	0.689	0.575 ± 0.134	4.76	6.3 × 10 ⁻⁵
		Yes	0.698	0.698 ± 0.017		
	VITA-Sinusoidal	No	0.684	0.569 ± 0.139	4.80	5.7 × 10 ⁻⁵
		Yes	0.722	0.698 ± 0.019		

Table 9: Pretraining effect across hyperparameter configurations during grid search. T-BERT evaluated over 9 configurations (3 learning rates × 3 batch sizes × 1 regularization value), VITA variants over 27 configurations (3 learning rates × 3 batch sizes × 3 β values). P-values from paired t-tests comparing pretrained vs non-pretrained.

Crop	Model	Pretrained	Best R ²	Mean R ²	t-statistic	p-value
Corn	VITA-Std	No	0.667	0.463 ± 0.230	3.82	7.5 × 10 ⁻⁴
		Non-US	0.662	0.632 ± 0.018		
	VITA-Sinusoidal	No	0.672	0.469 ± 0.227	3.61	1.3 × 10 ⁻³
		Non-US	0.658	0.627 ± 0.020		
Soybean	VITA-Std	No	0.689	0.575 ± 0.134	3.72	9.5 × 10 ⁻⁴
		Non-US	0.710	0.674 ± 0.020		
	VITA-Sinusoidal	No	0.684	0.569 ± 0.139	3.685	1.0 × 10 ⁻³
		Non-US	0.707	0.669 ± 0.021		

Table 10: Spatial transfer learning: pretraining on Central/South America (excluding continental US) across 27 hyperparameter configurations. P-values from paired t-tests comparing Non-US pretrained vs no pretraining.

OLS achieves only 0.227 R² for corn and 0.460 R² for soybean on extreme years (Table 1), demonstrating that linear assumptions and hand-crafted features fundamentally fail on unprecedented weather events. While the ERS framework was designed for stable conditions (Westcott and Jewison 2013), extreme weather requires capturing complex nonlinear interactions. VITA achieves 3.2× improvement over OLS for corn (0.729 vs 0.227 R²), confirming that learned representations are essential for climate-resilient yield prediction.

Lead Time Performance For operational forecasting, growers and insurers need yield estimates before harvest. Table 3 (main text) evaluates performance with end-of-July cutoff: 6 complete years (312 weeks) + 30 weeks of the target year, totaling 342 of 364 weeks (removing the final 22 weeks of August-December weather). This timing is critical in the US Corn Belt, as corn enters late grain fill and soybeans approach reproductive peak (Westcott and Jewison 2013).

VITA-Sinusoidal achieves 0.689 R² for corn and 0.560 R² for soybean with the July cutoff. Corn performance drops modestly (0.040 R²) while soybean drops substan-

tially (0.162 R²)—a biologically meaningful difference since August is the critical pod-filling period when weather directly determines soybean seed weight (Westcott and Jewison 2013). No weather forecasts were used; predictions rely solely on observed weather through July.

VITA-Sinusoidal still achieves 3.0× improvement over OLS for corn (0.689 vs 0.227) and 1.5× for soybean (0.560 vs 0.382) despite identical cutoffs. Importantly, VITA-Sinusoidal shows superior robustness: while SimMTM drops 0.096 R² (corn) and 0.204 R² (soybean), and T-BERT drops 0.071 R² (corn) and 0.185 R² (soybean), VITA-Sinusoidal degrades less (0.040 R² corn, 0.162 R² soybean), confirming its viability for pre-harvest operational forecasting.

Reduced Temporal Context To test data efficiency, we evaluate extreme years using only 5 years of weather history (260 weeks) instead of 7 years (364 weeks)—a 28% reduction with practical implications for data-scarce regions or faster inference. Table 13 shows VITA-Sinusoidal achieves 0.697 R² for corn and 0.684 R² for soybean, outperforming most baselines in Table 1 despite limited context.

Crop	Year	T-BERT R ² ± std	VITA-Sinusoidal R ² ± std
Corn	2002	0.694 ± 0.021	0.722 ± 0.011
	2004	0.670 ± 0.056	0.760 ± 0.036
	2009	0.846 ± 0.005	0.866 ± 0.002
	2012	0.347 ± 0.089	0.482 ± 0.031
	2014	0.745 ± 0.034	0.817 ± 0.010
Soybean	2003	0.484 ± 0.021	0.579 ± 0.013
	2004	0.676 ± 0.015	0.718 ± 0.005
	2009	0.773 ± 0.003	0.789 ± 0.015
	2012	0.712 ± 0.020	0.689 ± 0.003
	2016	0.820 ± 0.020	0.834 ± 0.002
Mean		0.677	0.726

Table 11: Detailed R² performance on extreme years for statistical analysis.

Crop	Prior	No-Pre. Best R ²	Pre. Best R ²	Δ
Corn	Std-Norm.	0.685	0.732	+0.047
	Sinusoidal	0.672	0.708	+0.036
Soybean	Std-Norm.	0.687	0.717	+0.030
	Sinusoidal	0.684	0.715	+0.031

Table 12: Year-permutation ablation on corn and soybean yield prediction. Pretraining benefits persist even when temporal relationships are destroyed.

Performance degradation is modest: corn drops 0.032 R² (sinusoidal) and soybean 0.038 R². The standard normal prior shows even greater robustness (0.040 R² drop for corn, 0.004 R² for soybean), indicating both variants effectively leverage available temporal information when context is limited.

Crop	VITA Prior	7 Years R ² (RMSE)	5 Years R ² (RMSE)
Corn	Std. Normal	0.706 ± 0.025 (17.1 ± 0.7)	0.666 (18.2)
	Sinusoidal	0.729 ± 0.008 (16.3 ± 0.2)	0.697 (17.4)
Soybean	Std. Normal	0.698 ± 0.020 (5.2 ± 0.2)	0.694 (5.3)
	Sinusoidal	0.722 ± 0.005 (5.0 ± 0.1)	0.684 (5.3)

Table 13: Reduced temporal context on extreme years: 5 years (260 weeks) vs 7 years (364 weeks) of weather data.

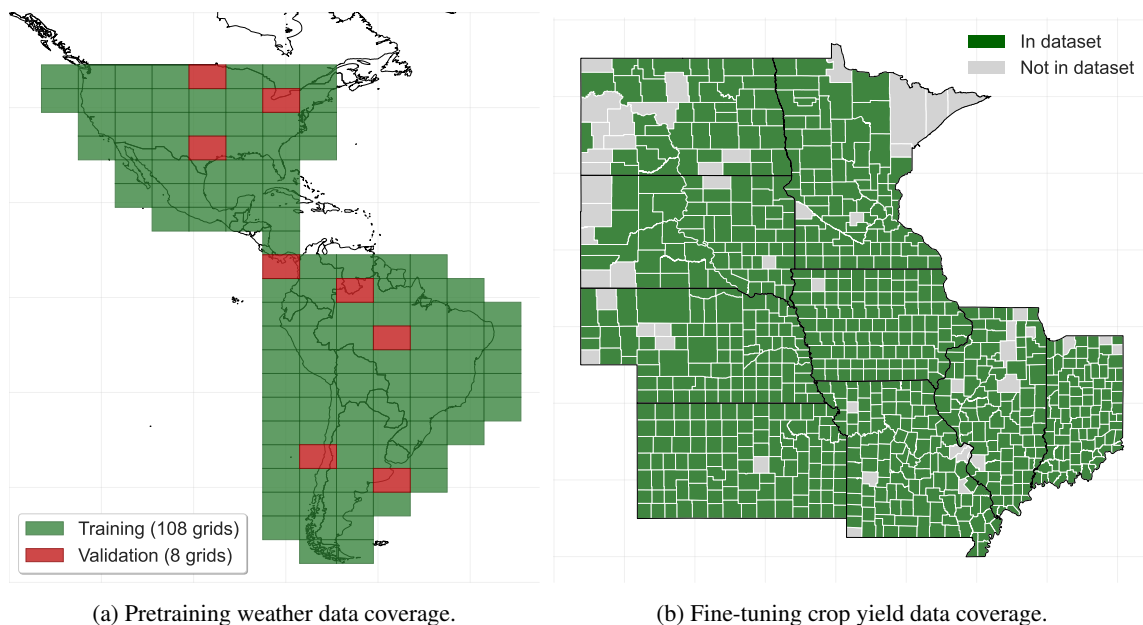


Figure 7: Spatial coverage of pretraining and fine-tuning datasets.

Measurement Name	Symbol	Unit
Temperature at 2 Meters	T2M	°C
Temperature at 2 Meters Maximum	T2M_MAX	°C
Temperature at 2 Meters Minimum	T2M_MIN	°C
Wind Direction at 2 Meters	WD2M	Degrees
Wind Speed at 2 Meters	WS2M	m/s
Surface Pressure	PS	kPa
Specific Humidity at 2 Meters	QV2M	g/Kg
Precipitation Corrected	PRECTOTCORR	mm/day
All Sky Surface Shortwave Downward Irradiance	ALLSKY_SFC_SW_DWN	MJ/m ² /day
Evapotranspiration Energy Flux	EVPTRNS	MJ/m ² /day
Profile Soil Moisture (0 to 1)	GWETPROF	0 to 1
Snow Depth	SNODP	cm
Dew/Frost Point at 2 Meters	T2MDEW	°C
Cloud Amount	CLOUD_AMT	0 to 1
Evaporation Land	EVLAND	kg/m ² /s × 10 ⁶
Wet Bulb Temperature at 2 Meters	T2MWET	°C
Land Snowcover Fraction	FRSNO	0 to 1
All Sky Surface Longwave Downward Irradiance	ALLSKY_SFC_LW_DWN	MJ/m ² /day
All Sky Surface PAR Total	ALLSKY_SFC_PAR_TOT	MJ/m ² /day
All Sky Surface Albedo	ALLSKY_SRF_ALB	0 to 1
Precipitable Water	PW	cm
Surface Roughness	Z0M	m
Surface Air Density	RHOA	kg/m ³
Relative Humidity at 2 Meters	RH2M	0 to 1
Cooling Degree Days Above 18.3 C	CDD18_3	days
Heating Degree Days Below 18.3 C	HDD18_3	days
Total Column Ozone	TO3	Dobson units
Aerosol Optical Depth 55	AOD_55	0 to 1
Reference Evapotranspiration	ET0	mm/day
Vapor Pressure	VAP	kPa
Vapor Pressure Deficit	VAD	kPa

Table 14: Descriptions of the 31 weather measurements and their units.